Facile and Restricted Pathways for the Dissociation of Octenoyl-CoA from the Medium-Chain Fatty Acyl-CoA Dehydrogenase (MCAD)-$FADH_2$−Octenoyl-CoA Charge-Transfer Complex: Energetics and Mechanism of Suppression of the Enzyme's Oxidase Activity†

N. Ravi Kumar and D. K. Srivastava*

Biochemistry Department, North Dakota State University, Fargo, North Dakota 58105

Received February 23, 1995; Revised Manuscript Received May 24, 1995®

ABSTRACT: In a previous paper, we demonstrated that the reductive half-reaction of medium-chain fatty acyl-CoA dehydrogenase (MCAD), utilizing octanoyl-CoA as physiological substrate, generates two (kinetically distinct) forms of the reduced enzyme (MCAD-$FADH_2$)−octenoyl-CoA charge-transfer complexes [Kumar, N. R., & Srivastava, D. K. (1994) *Biochemistry 33*, 8833−8841]. We present evidence that octenoyl-CoA dissociates from the second (most stable) charge-transfer complex (referred to as CT_2) via two alternative ("facile" and "restricted") pathways. The dissociation of octenoyl-CoA via the facile pathway involves the reversal of the overall reductive half-reaction of the enzyme, generating MCAD-FAD−octanoyl-CoA as the Michaelis complex, followed by dissociation of the latter complex into MCAD-FAD + octanoyl-CoA. Hence, via this pathway, octenoyl-CoA is released from the enzyme site in the form of octanoyl-CoA. In contrast, the restricted pathway involves a direct (albeit slow) dissociation of octenoyl-CoA from CT_2 to yield MCAD-$FADH_2$ + octenoyl-CoA. The kinetic profile for the dissociation of octenoyl-CoA via the restricted pathway matches the rate of oxidation of the reduced flavin (within CT_2) by O_2. This suggests that the oxidase activity of the enzyme remains suppressed as long as the reduced enzyme predominates in the form of the charge-transfer complex(es). The oxidase activity of the enzyme emerges concomitantly with the conversion of CT_2 to the MCAD-$FADH_2$−octenoyl-CoA Michaelis complex. The energetic basis for the dissociation of octenoyl-CoA via the facile and restricted pathways and the mechanism of suppression of the oxidase activity of the enzyme are discussed.

In a series of publications, over the past four years, we have investigated various aspects of the mechanism of medium-chain fatty acyl-CoA dehydrogenase (MCAD)[1] catalyzed reactions (Johnson et al., 1992, 1993, 1994; Johnson & Srivastava, 1993; Kumar & Srivastava, 1994; Srivastava et al., 1995). This enzyme is involved in the β-oxidative pathway of the mitochondrial matrix and catalyzes the oxidation of various fatty acyl-CoAs into their corresponding enoyl-CoAs via two distinct steps [for reviews, see Beinert (1963a) and Engel (1990)]. The first step, conventionally known as the "reductive half-reaction", involves the reduction of the enzyme-bound flavin with concomitant removal of α and β hydrogens from the acyl-CoA substrates (Ghisla et al., 1984; Frerman et al., 1980). The repetitive turnover of the enzyme is maintained via reoxidation of the reduced flavin by a variety of organic electron acceptors during the second "oxidative half-reaction" (Lehman & Thorpe, 1990). The physiological electron acceptor of the enzyme is the electron-transferring flavoprotein (ETF-FAD; Beinert, 1963b).

Our understanding of the MCAD-catalyzed reaction mechanism began to be refined while utilizing indolepropionyl-CoA (IPCoA) and indoleacryloyl-CoA (IACoA) as a chromogenic substrate/product pair, respectively (Johnson et al., 1992). Due to the characteristic absorption spectrum of IACoA (absorption maximum = 367 nm), we could easily monitor the kinetics of the enzyme-catalyzed reaction, as well as probe the enzyme site environment (Johnson et al., 1992, 1994; Johnson & Srivastava, 1993; Srivastava et al., 1995). The chromophoric potential of IACoA allowed us to detect an intermediary species (absorption maximum = 400 nm), designated as "X", during the IPCoA-dependent reductive half-reaction of the enzyme (Johnson & Srivastava, 1993). This intermediary species also exhibited the property of the charge-transfer complex band, formed with all the acyl-CoA substrates examined so far (Engel, 1990). Also, the kinetic profiles for the formation and decay of X were found to be same irrespective of whether the reaction progress was monitored in the oxidized flavin region (i.e., at 400 nm) or in the charge transfer complex region (i.e., 507−800 nm) (Johnson & Srivastava, 1993). Since a similar intermediary species (characterized by the charge transfer complex band, but devoid of the 400-nm absorption band) is formed during the butyryl-CoA-dependent reductive half-reaction of the enzyme (Schopfer et al., 1988; Johnson & Srivastava 1993), it is evident that the origin of the 400-nm absorption band

† Suppported by a standard grant-in-aid from the American Heart Association, Dakota Affiliate, Inc.

* To whom correspondence should be addressed.

® Abstract published in *Advance ACS Abstracts,* July 15, 1995.

[1] Abbreviations: MCAD, medium-chain fatty acyl-CoA dehydrogenase; IPCoA, 3-indolepropionyl coenzyme A; IACoA, *trans*-3-indoleacryloyl coenzyme A; BuCoA, Butyryl coenzyme A; FAD, flavin adenine dinucleotide; $FADH_2$, reduced flavin adenine dinucleotide; ETF, electron-transferring flavoprotein; CoA, coenzyme A; OcaCoA, octanoyl-CoA; OceCoA; octenoyl-CoA; AcAcCoA, acetoacetyl-CoA; CT, charge-transfer complex; $FcPF_6$, ferrocenium hexafluorophosphate.

0006-2960/95/0434-9434$09.00/0

(in the case of IPCoA) lies in the chromophoric nature of the reaction product IACoA (Johnson & Srivastava, 1993; Johnson et al., 1993). Hence, X is indeed a charge transfer containing intermediary species, and it is formed with different types of acyl-CoA substrates.

We recently deduced that, unlike the reductive half-reaction with IPCoA or butyryl-CoA, the octanoyl-CoA-dependent reductive half-reaction of the enzyme involves the formation of two (instead of one) intermediary enzyme species that exhibit the property of charge-transfer complex (Kumar & Srivastava, 1994). With analogy to the IPCoA/butyryl-CoA-dependent reactions (see above), we assigned these species as X and X′. Realizing that this assignment is causing unnecessary confusion, we have opted to refer to all intermediary species as the charge-transfer (CT) complexes. Hence, in the case of butyryl-CoA and IPCoA, the intermediary species (*one* in existence) will be referred to as CT, whereas in the case of octanoyl-CoA, the intermediary species (*two* in existence) will be referred to as CT_1 and CT_2, respectively (eq 1). Since the equilibrium distribution among

$$\begin{aligned}&\text{E-FAD + OcaCoA} \rightleftharpoons \text{E-FAD-OcaCoA} \rightleftharpoons \\ &\quad \text{CT}_1\ (\text{E-FADH}_2\text{-OceCoA})^{*} \rightleftharpoons \text{CT}_2\ (\text{E-FADH}_2\text{-OceCoA})^{**}\end{aligned}$$

$$\text{E-FAD + IPCoA} \rightleftharpoons \text{E-FAD-IPCoA} \rightleftharpoons \text{CT}\ (\text{E-FADH}_2\text{-IACoA})^{*} \quad (1)$$

different enzyme species is substantially in favor of CT_2, the latter is almost a sole representative of the charge-transfer complexes, formed with octanoyl-CoA (Kumar & Srivastava, 1994).

While investigating the IPCoA-dependent reaction of MCAD, we observed that the intermediary species, CT (formerly designated as X), decays/collapses under the influence of an excessive concentration of the substrate (Johnson & Srivastava, 1993; Johnson et al., 1994). Circumstantial evidence corroborated the notion that the stability of the intermediary complex was responsible for dictating the "dehydrogenase" versus the "oxidase" activity of the enzyme (Johnson et al., 1994; Srivastava et al., 1995). Whereas the rate of formation of CT was found to limit the turnover rate of the MCAD-catalyzed dehydrogenase reaction, the rate of decay of CT was found to limit the turnover rate of the oxidase reaction (Johnson & Srivastava, 1993; Johnson et al., 1994; eq 2).

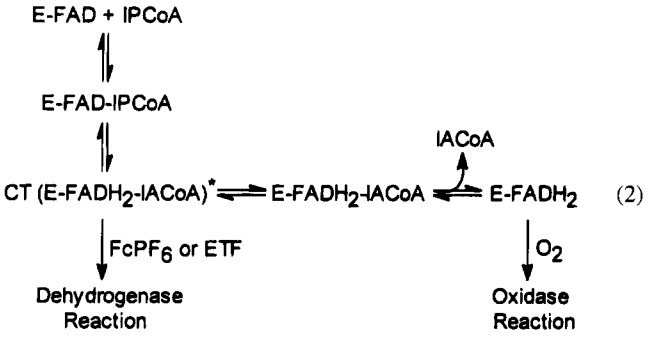

(2)

We considered whether this conclusion is unique only for the substrate IPCoA or it applies to other acyl-CoA substrates, particularly octanoyl-CoA, which has been recognized to be a physiological substrate for this enzyme (Hall et al., 1979; Engel, 1990). As will be elaborated in this paper, despite the difference in the microscopic pathways between IPCoA- and octanoyl-CoA-dependent reductive half-reactions of the enzyme (Kumar & Srivastava, 1994), the origin of the oxidase activity conforms to a common mechanistic principle.

MATERIALS AND METHODS

Materials. Coenzyme A, octanoyl-CoA, acetoacetyl-CoA, and glucose oxidase were purchased from Sigma. All other reagents were of analytical grade.

Methods. All experiments were performed in a standard 50 mM potassium phosphate buffer (pH 7.6) containing 0.3 mM EDTA at 25 °C, unless stated otherwise. Anaerobic experiments were performed as described by Kumar and Srivastava (1994).

Pig kidney MCAD was purified in our laboratory and assayed as described by Johnson et al. (1992). The concentration of MCAD was determined in terms of flavin content by using an extinction coefficient of 15.4 mM^{-1} cm^{-1} at 446 nm (Thorpe et al., 1979).

Octenoyl-CoA was prepared and purified as described by Kumar and Srivastava (1994). IACoA was prepared by the mixed-anhydride method of Bernert and Sprecher (1977) and purified as described by Johnson et al. (1992). The concentrations of octenoyl-CoA and IACoA were determined by using extinction coefficients of 20.4 mM^{-1} cm^{-1} (258 nm; Kumar & Srivastava, 1994) and 26.5 mM^{-1} cm^{-1} (367 nm; Johnson et al., 1992), respectively. The extinction coefficient of both acetoacetyl-CoA and octanoyl-CoA was taken to be 15.6 mM^{-1} cm^{-1} at 259 nm.

Spectral acquisitions and steady-state kinetic experiments were performed on a Beckman 7400 diode-array spectrophotometer or on Perkin-Elmer (lambda-3B) dual-beam spectrophotometers.

Transient Kinetic Experiments. The transient kinetic experiments were performed on an Applied Photophysics MV-14 sequential-mixing stopped-flow system (optical path length = 10 mm; dead time = 1.34 ms). The experimental results presented herein were obtained by configuring our stopped-flow device in a single mixing mode. In this mode, the contents of syringes A and B were diluted by 50%. The stopped-flow kinetic traces were analyzed by the data analysis package provided by Applied Photophysics.

Numerical Simulations. The MCAD-catalyzed reaction mechanism was numerically simulated using the program PLOD of D. K. Kahaner and D. D. Barnet (Center for Computing and Applied Mathematics, National Institute of Standards and Technology, Gaithersburg, MD 20899) as described by Betts and Srivastava (1991). Since PLOD uses Gear algorithm, the dissociation constants (K_ds) for the enzyme−ligand complexes were translated into the association (k_{on}) and dissociation (k_{off}) rate constants ($K_d = k_{off}/k_{on}$). Assuming that the enzyme−ligand interaction is a diffusion-limited process, the magnitude of k_{on} is taken to be 1×10^9 M^{-1} s^{-1}. The simulated traces were analyzed according to single- or double-exponential rate equations by Enzfitter.

Construction of the Gibbs' Free Energy Profile for the Octanoyl-CoA-Dependent Reductive Half-Reaction of the Enzyme. The Gibbs' free energy profile of Figure 5 was constructed by calculating the free energies of the ground and transition states of the individual enzyme-bound species (formed during the reductive half-reaction of the enzyme) according to standard thermodynamic equations (Fersht, 1985). The rate and equilibrium constants of Table 1 were

utilized in these calculations. The standard state for both octanoyl-CoA and octenoyl-CoA was taken to be 1 M. The reference state for MCAD-FAD was taken to be zero. Following are the relationships between Gibbs' free energy of the individual enzyme species and their associated rate and equilibrium constants.

$$G_{\text{MCAD-FAD}} = 0$$

$$G_{\text{MCAD-FAD-OcaCoA}} = RT \ln K_s$$

$$G_{(\text{MCAD-FAD-OcaCoA})}^{\ddagger} = RT \ln(k_B T/h) - RT \ln(k_3/K_s)$$

$$G_{CT_1} = -RT \ln(k_3/k_4 K_s)$$

$$G_{CT_1}^{\ddagger} = RT \ln(k_B T/h) - RT \ln(k_3 k_5/k_4 K_s)$$

$$G_{CT_2} = -RT \ln(k_3 k_5/k_4 k_6 K_s)$$

$$G_{CT_2}^{\ddagger} = RT \ln(k_B T/h) - RT \ln(k_3 k_5 k_7/k_4 k_6 K_s)$$

$$G_{\text{MCAD-FADH}_2\text{-OceCoA}} = -RT \ln(k_3 k_5 k_7/k_4 k_6 k_8 K_s)$$

$$G_{\text{MCAD-FADH}_2} = -RT \ln(k_3 k_5 k_7 K_p/k_4 k_6 k_8 K_s)$$

where R is the gas constant (8.31 J K^{-1} mol^{-1}), T is the absolute temperature (298 K), k_B is Boltzmann's constant (1.38×10^{-23} J K^{-1}), and h is Plank's constant (6.63×10^{-34} J s).

Theory for Determining the Dissociation Constant of the MCAD-FAD−Octanoyl-CoA Complex. If two ligands (A and B) compete for an enzyme site (E), it is intuitively obvious that the dissociation constant for the EA complex can be determined if the dissociation constant for the EB complex is already known. Such a determination is relatively easy if $[E]_{total} \ll K_d(A)$ and $K_d(B)$, and $[E]_{total} \ll [A]_{total}$ and $[B]_{total}$. Under this situation, the total concentrations of the ligands can be taken as being equal to their free concentrations. On the other hand, if this ideal situation is not satisfied, and the enzyme−ligand dissociation constants are comparable to the initial concentrations of the enzyme and ligands, the dissociation constant determination becomes somewhat cumbersome. In the following paragraphs, we provide a relatively simple analytical method for determining the dissociation constant of an enzyme−ligand (EA) complex ($K_d(A) \leq [E]_{total}$) in the presence of a competitive ligand (B) with a considerably higher dissociation constant ($K_d(B) > [E]_{total}$). We must point out that this method is not applicable in cases where the dissociation constants for both ligands (i.e., $K_d(A)$ and $K_d(B)$) are fairly low (i.e., in the nanomolar range).

Consider an equilibrium reaction between an enzyme and its two competitive ligands, A and B, with dissociation constants of EA and EB complexes of K_a and K_b (where $K_a \ll K_b$), respectively (eq 3):

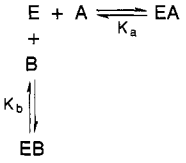

(3)

If the free and total concentrations of E, A, and B are represented by [E], [A], and [B] and $[E]_t$, $[A]_t$, and $[B]_t$, respectively, K_a and K_b can be represented as follows:

$$K_a = [E][A]/[EA] = [E]([A]_t - [EA])/[EA] \quad (4)$$

$$K_b = [E][B]/[EB] = [E]([B]_t - [EB])/[EB] \quad (5)$$

If $[E]_t \ll [B]_t$, then $[B]_t$ can be taken to be equal to [B]. Under this situation,

$$[EA] = [E][A]_t/(K_a + [E]) \quad \text{and} \quad [E] = K_b[EB]/[B]_t \quad (6)$$

According to mass balance,

$$[E]_t = [E] + [EA] + [EB] \quad (7)$$

Upon substituting the values of [E] and [EA] from eq 6 in eq 7, we obtain

$$[E]_t = [EB]\{1 + K_b/[B]_t\} + [E][A]_t/(K_a + [E]) \quad (8)$$

A quadratic solution of eq 8 yields the following relationship:

$$[EB] = 0.5\{-b + \sqrt{(b^2 + 4c)}\} \quad (9)$$

where

$$b = \frac{K_a[B]_t}{K_b} + \frac{[B]_t([A]_t - [E]_t)}{K_b + [B]_t}$$

and

$$c = \frac{K_a[E]_t[B]_t[B]_t}{K_b(K_b + [B]_t)}$$

Given the initial concentrations of $[E]_t$ and $[A]_t$ and the independently determined parameter K_b, the magnitude of K_a can be determined (according to eq 9) by measuring the amount of EB at increasing concentrations of B_t. If EB is characterized by an absorption signal (absorbance = $\epsilon_{EB} \times [EB]$), this determination can be made by measuring the absorption changes due to EB as a function of B_t. This stratagem has been employed for determining the dissociation constant of the MCAD-FAD−octanoyl-CoA complex by titrating a reaction mixture of MCAD-FAD and octanoyl-CoA (which is predominantly converted into the MCAD-$FADH_2$−octenoyl-CoA charge-transfer complex, CT_2) with increasing concentrations of either acetoacetyl-CoA or IA-CoA (see below).

Determination of the Dissociation Constant of MCAD-FAD−Acetoacetyl-CoA Complex. The dissociation constant of the MCAD-FAD−acetoacetyl-CoA complex was determined by adopting the titration protocol recently developed in our laboratory (Wang et al., 1992). Unlike the conventional method (Fersht, 1985), this method is limited neither to the range of enzyme or ligand concentrations nor to the extent of spectral changes upon formation of the enzyme−ligand complexes (Wang et al., 1992). As per our titration protocol, a fixed concentration of MCAD-FAD was titrated with increasing aliquots of a fixed concentration of stock solution of acetoacetyl-CoA, and the absorbance spectra were recorded after each addition. A plot of absorption changes at 545 nm versus the volume of acetoacetyl-CoA was made. The dissociation constant of the enzyme−acetoacetyl-CoA

complex was determined by analyzing the experimental data as described by Wang et al. (1992).

Titration of MCAD-FADH$_2$−Octenoyl-CoA Charge-Transfer Complex (CT_2) by Acetoacetyl-CoA and IACoA. A limiting concentration of MCAD-FADH$_2$−octenoyl-CoA charge-transfer complex CT_2 (prepared by mixing 12 μM octanoyl-CoA and 10 μM MCAD-FAD in a total volume of 1.0 mL) was titrated with increasing concentrations of either acetoacetyl-CoA or IACoA. The spectra of the reaction mixtures were acquired (on a Beckman-7400 diode-array spectrophotometer) during the course of this titration. The difference spectra were generated after subtracting the contributions of the individual species from the spectra of the mixtures. The absorption slices (440 nm in the case of acetoacetyl-CoA and 450 nm in the case of IACoA), taken from these spectra, were plotted against the total concentrations of the respective CoA ligands. The data were analyzed according to eq 9 by Enzfitter.

RESULTS

In order to construct a quantitative model for the octanoyl-CoA-dependent MCAD-catalyzed reaction, we performed all experiments at 25 °C, in 50 mM phosphate buffer, pH 7.6, containing 0.3 mM EDTA.

We measured the transient courses for the reaction of MCAD-FAD and octanoyl-CoA ([MCAD-FAD] ≪ [octanoyl-CoA]) at different concentrations of octanoyl-CoA at 450 and 565 nm (data not shown). As observed at 5 °C (Kumar & Srivastava, 1994), the reaction profiles were found to be consistent with a biphasic decrease in absorbance at 450 nm, and a biphasic increase in absorbance at 565 nm. The average values of the fast and slow relaxation rate constants (at 25 °C) were found to be 649 ± 19.1 and 66.5 ± 5.1 s^{-1}, respectively. These values are approximately 2-fold higher than those obtained at 5 °C, and both of these phases showed apparent zero-order dependence on the octanoyl-CoA concentration (under pseudo-first-order conditions). Under neither of the above conditions did we observe any additional phases, in particular a slow third phase of rate constant about 5 s^{-1} as reported by Lau et al. [see Table 2 of Lau et al. (1989)], during the octanoyl-CoA-dependent reductive half-reaction of the enzyme. We offer no explanation for this discrepancy.

We also measured the transient course for the reaction of MCAD-FAD + octenoyl-CoA ([MCAD-FAD] ≪ [octenoyl-CoA]) at 25 °C by following the absorption changes at 299 nm (Kumar & Srivastava, 1994). Consistent with our earlier results at 5 °C (Kumar & Srivastava, 1994), this reaction was also found to be biphasic (data not shown), with average fast and slow relaxation rate constants of 661 ± 71.6 and 26.2 ± 1.8 s^{-1}, respectively. These rate constants are once again 2-fold higher than those determined at 5 °C, and both of these phases exhibit apparent zero-order dependence on the octenoyl-CoA concentration (under pseudo-first-order conditions).

While maintaining anaerobic conditions, we performed the transient kinetic experiments for the reaction of MCAD-FADH$_2$ (generated by reduction of MCAD-FAD by sodium dithionite) and octenoyl-CoA (data not shown). The reaction progress was found to be consistent with a biphasic increase in absorbance at 450 nm (the oxidized flavin region) and an increase followed by a decrease in absorbance at 565 nm (the charge-transfer complex region). These relaxation rate constants were found to be independent of octenoyl-CoA concentration (under pseudo-first-order conditions), with average fast and slow relaxation rate constants at 25 °C of 757 ± 32.6 and 3.5 ± 0.18 s^{-1}, respectively. A detailed account of the reverse reaction will be published subsequently.

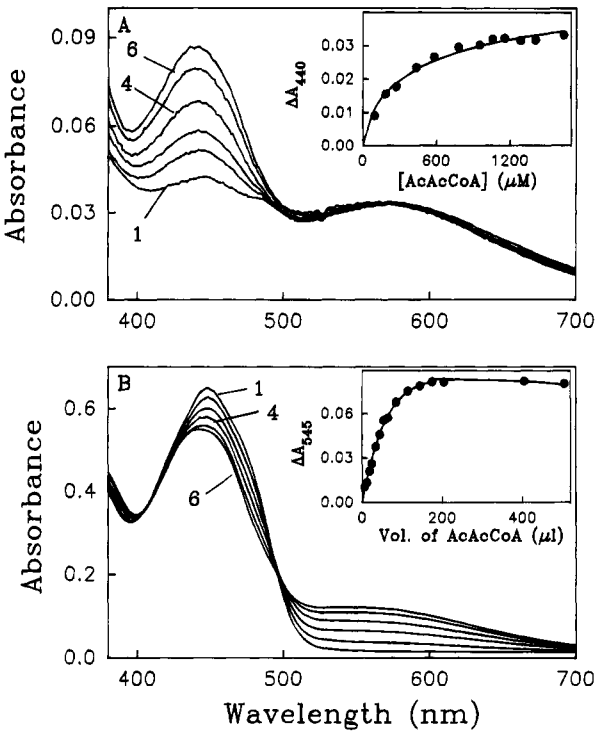

FIGURE 1: Panel A: Effect of acetoacetyl-CoA on the spectral properties of the octanoyl-CoA-reduced enzyme (charge-transfer complex, CT_2). [MCAD-FAD] = 10 μM; [octanoyl-CoA] = 12 μM. The concentrations of acetoacetyl-CoA for spectra 1−6 are 0, 96.1, 187.3, 435.3, 779, and 1057 μM, respectively. The inset shows the increase in absorbance at 440 nm as a function of the total concentration of acetoacetyl-CoA. The solid line is the best fit of the experimental data (according to eq 9) for an equilibrium dissociation constant of CT_2 ⇌ MCAD-FAD + octanoyl-CoA of 0.180 μM. Panel B: Titration of MCAD-FAD with acetoacetyl-CoA. Spectral changes during the course of titration of a fixed concentration of MCAD-FAD (42.0 μM, spectrum 1) with increasing volumes of a 600 μM stock solution of acetoacetyl-CoA (spectra 2−6) are shown. The absorption of MCAD-FAD is corrected for dilution. The inset shows a plot of the absorption changes at 545 nm against the total volume of acetoacetyl-CoA. The decrease in absorption at 545 nm is due to the dilution effect of the increasing volumes of acetoacetyl-CoA on the MCAD-FAD−acetoacetyl-CoA complex yield. The solid line is the best fit of the experimental data according to Wang et al. (1992) with a dissociation constant of 12.6 ± 0.9 μM.

Effects of Acetoacetyl-CoA and IACoA on the Spectral Properties of MCAD-FADH$_2$−Octenoyl-CoA Charge-Transfer Complex (CT_2). It has been established that, even in the presence of stoichiometric ratios of octanoyl-CoA to MCAD-FAD (both present in the micromolar range), about 85−90% of the enzyme-bound FAD is reduced to FADH$_2$ (Beinert & Page, 1957; Kumar & Srivastava, 1994). This process occurs concomitantly with conversion of the enzyme-bound octanoyl-CoA to octenoyl-CoA, and the resultant complex exhibits properties of the charge-transfer band (CT_2; Engel, 1990).

We considered the feasibility of displacement of octenoyl-CoA from CT_2 in the presence of excessive concentrations of CoA analogues, e.g., acetoacetyl-CoA or IACoA. Figure 1A shows the effects of increasing concentrations of ac-

etoacetyl-CoA on the spectral properties of CT_2 under aerobic conditions. The spectral data of Figure 1A reveals that as the concentration of acetoacetyl-CoA increases, the 450-nm flavin band increases, whereas the charge transfer complex band remains minimally affected. At a saturating concentration of acetoacetyl-CoA (i.e., 1600 μM; see below), the spectrum of the mixture resembles that of the oxidized enzyme−acetoacetyl-CoA complex (see Figure 1B). The latter feature is explicitly evident from the acetoacetyl-CoA concentration-dependent spectral changes of MCAD-FAD. As shown in Figure 1B, as the concentration of acetoacetyl-CoA increases, the absorption band at 450 nm slightly decreases. The latter proceeds concomitantly with the appearance of the charge transfer complex band (presumably where the enolate form of acetoacetyl-CoA serves as the electron donor and FAD serves as the electron acceptor) with an absorption maximum around 545 nm. This band is qualitatively similar to that formed during the octanoyl-CoA-dependent reductive half-reaction of the enzyme (albeit in this case $FADH_2$ serves as the electron donor and octenoyl-CoA serves as the electron acceptor). The inset of Figure 1B shows the absorbance changes at 545 nm upon titration of a limiting concentration of MCAD-FAD (42 μM) with increasing volumes of a stock solution of acetoacetyl-CoA (600 μM) as described by Wang et al. (1992). Note that as the volume of acetoacetyl-CoA increases, the absorption at 545 nm first increases, attains a maximum value, and then starts decreasing due to the dilution effect. The solid line is the best fit of the experimental data according to Wang et al. (1992) for the dissociation constant of MCAD-FAD−acetoacetyl-CoA complex to be 12.6 ± 0.9 μM.

A cumulative account of these results led us to consider that the spectral changes of Figure 1A might have arisen due to competitive displacement of octenoyl-CoA from CT_2 by acetoacetyl-CoA, followed by oxidation of the resulting complex (eq 10).

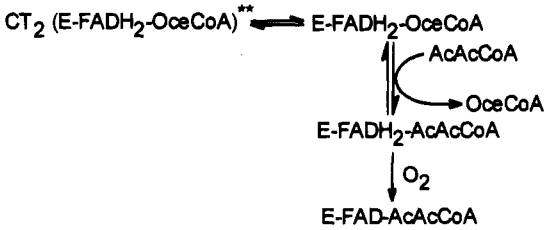

(10)

This possibility was negated by the fact that the spectral changes remained invariant irrespective of whether the reaction was performed under aerobic or anaerobic conditions (data not shown). This prompted us to consider that the acetoacetyl-CoA concentration-dependent spectral changes of Figure 1A are due to the reversal of the overall reductive half-reaction of the enzyme (eq 11).

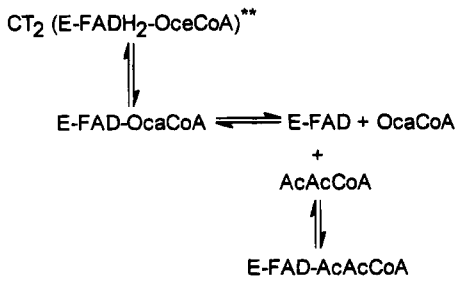

(11)

In eq 11 (as well as in eqs 12 and 13), we have considered

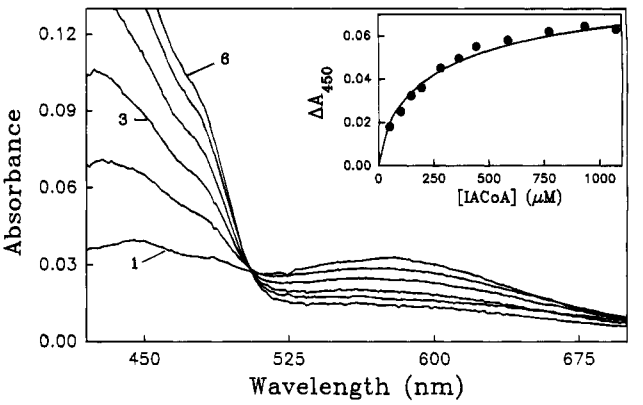

FIGURE 2: Effect of IACoA on the spectral properties of the octanoyl-CoA-reduced enzyme (charge-transfer complex, CT_2). [MCAD-FAD] = 10 μM MCAD-FAD; [octanoyl-CoA] = 12 μM. The concentrations of IACoA for spectra 1−6 are 0, 99.7, 281, 584.6, 934.2, and 1236 μM, respectively. The inset shows the increase in absorbance at 450 nm (corrected for the dilution of the individual species) as a function of the total concentration of IACoA. The solid line is the best fit of the experimental data (according to eq 9) for an equilibrium dissociation constant of CT_2 ⇌ MCAD-FAD + octanoyl-CoA of 0.073 μM.

CT_2 as the sole charge-transfer complex species, since the equilibrium distribution between MCAD-FAD−octanoyl-CoA and CT_1 is close to unity, and that between CT_1 and CT_2 is predominantly in favor of CT_2 (Kumar & Srivastava, 1994; see Figure 5). In addition, for the sake of simplicity, we have represented the MCAD-FAD + CoA ligand (where the CoA ligand is either acetoacetyl-CoA, IACoA, or octenoyl-CoA) interactions as *one-* rather than *two-* or *three-*step processes (see Discussion).

The possibility of reversal of the reductive half-reaction as depicted by eq 11 was confirmed by performing a similar titration experiment (as in Figure 1A) utilizing IACoA as a competitive ligand. This is because the spectral properties of IACoA are remarkably different when it is bound to MCAD-FAD versus MCAD-$FADH_2$ sites (Johnson et al., 1992). Figure 2 shows the spectral changes of CT_2 in the presence of increasing concentrations of IACoA. It is noteworthy that, like acetoacetyl-CoA, the increase in IACoA results in an increase in absorption in the oxidized flavin region (i.e., around 450 nm). However, unlike that of acetoacetyl-CoA, the charge-transfer band of CT_2 starts disappearing at increasing concentrations of IACoA, and the resultant spectra resemble more the stable form (the form in which the electronic structures of both FAD are IACoA are perturbed) of the MCAD-FAD−IACoA complex, rather than that of the MCAD-$FADH_2$−IACoA complex (Johnson et al., 1992). Consistent with our acetoacetyl-CoA titration results (Figure 1A), the spectral profiles remained unaltered irrespective of whether the reaction condition was aerobic or anaerobic. These results provide strong support for the reversal of the octanoyl-CoA-dependent reductive half-reaction of the enzyme in the presence of CoA ligands, e.g., acetoacetyl-CoA or IACoA (eq 12).

The insets of Figures 1A and 2 show acetoacetyl-CoA- and IACoA-dependent absorption slices of the corresponding spectral data, respectively. The solid lines are the best fits of the experimental data according to the model presented in Materials and Methods (eq 9). Taking into account that the observed dissociation constants for the MCAD-FAD−IACoA and MCAD-FAD−acetoacetyl-CoA complexes are 2.7 ± 0.4 (Johnson et al., 1992) and 12.6 ± 0.9 μM (see

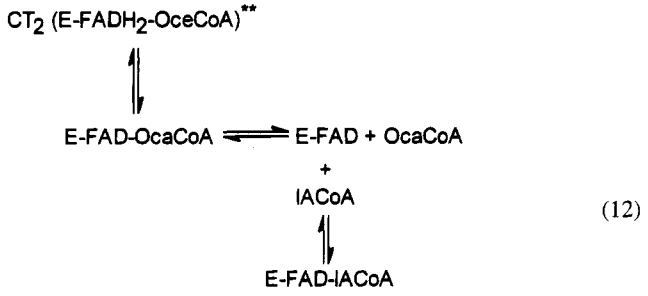

(12)

above), respectively, we could calculate the equilibrium constant for the conversion of CT_2 to MCAD-FAD + octanoyl-CoA. This value was found to be 180 ± 38 nM when acetoacetyl-CoA was utilized as a competitive ligand, and 73 ± 13 nM when IACoA was utilized as a competitive ligand. Although these values differ only by a factor of 2.5, the equilibrium dissociation constant obtained from the acetoacetyl-CoA-dependent titration results is taken to be more reliable. This is particularly so since at all the titration points (inset of Figure 1A) the total concentration of acetoacetyl-CoA can be taken to be equal to its free concentration. The latter satisfies one of the conditions for the quantitative evaluation of the above equilibrium constant by eq 9 (see theory in Materials and Methods).

It should be pointed out that the calculated equilibrium dissociation constant of 180 nM is indeed a product of two consecutive equilibria (eqs 11 and 12), i.e., $CT_2 \rightleftharpoons$ MCAD-FAD−octanoyl-CoA (chemical step) and MCAD-FAD−octanoyl-CoA $\rightleftharpoons$ MCAD-FAD + octanoyl-CoA (physical step). Given that the former is 1/8.5 (based on 85% reduction of MCAD-FAD by octanoyl-CoA), the latter can be calculated to be 1.53 μM. This value is similar to the K_m for octanoyl-CoA (2.0 ± 0.2 μM, our unpublished results) during the MCAD-catalyzed dehydrogenase reaction.

Kinetic Pathway for the Conversion of the Charge-Transfer Complex CT_2 to MCAD-FAD−Octanoyl-CoA Michaelis Complex, Followed by the Dissociation of Octanoyl-CoA. Given the characteristic spectral signals of Figures 1A and 2, we were able to measure the rate of reversal of the octanoyl-CoA-dependent reductive half-reaction of the enzyme (i.e., $CT_2 \rightarrow$ MCAD-FAD + octanoyl-CoA). This was accomplished by mixing a limiting concentration of CT_2 (prepared by mixing MCAD-FAD with octanoyl-CoA just prior to the experiment) with an excessive concentration of acetoacetyl-CoA (Figure 3A) or IACoA (Figure 3B). The solid smooth lines in these figures are the best fits of the experimental data according to the first-order rate law. The rate constants derived from the data of panels A and B of Figure 3 were 7.1 ± 0.1 and 5.4 ± 0.03 s^{-1}, respectively. Since the equilibration rate constants for the MCAD-FAD + octanoyl-CoA $\rightleftharpoons$ MCAD-FAD−octanoyl-CoA and MCAD-FAD + acetoacetyl-CoA/IACoA $\rightleftharpoons$ MCAD-FAD−acetoacetyl-CoA/IACoA reactions (under our experimental condition) are >10 000 s^{-1}, the observed rate constants of Figure 3 are expected to be primarily dominated by the slowest step (i.e., k_6 of Scheme 1) of the overall reaction pathway leading to the conversion of CT_2 to MCAD-FAD + octanoyl-CoA. However, depending upon the complexity of the reaction pathways, as well as the spectral properties of the intermediary enzyme species, the observed rate constants may contain contributions from steps other than k_6. This is presumably the reason for about 2-fold

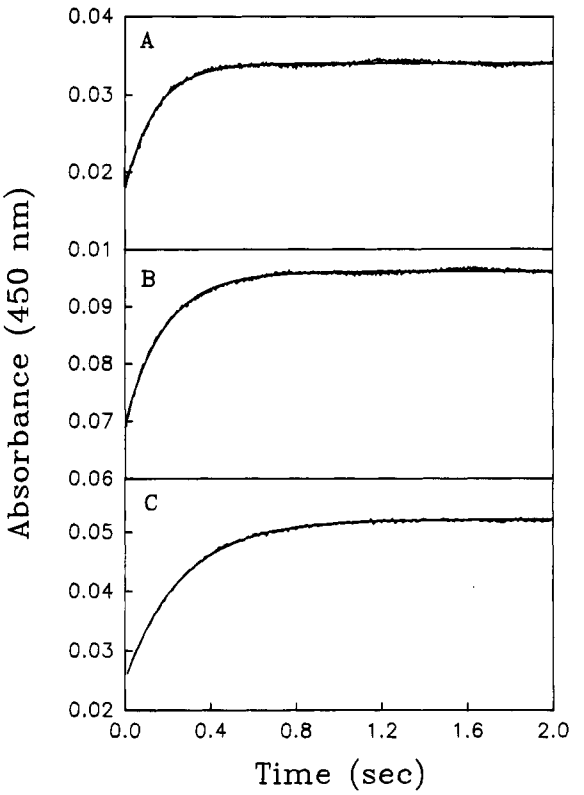

FIGURE 3: Representative stopped-flow traces (increase in absorption at 450 nm) for the dissociation of octenoyl-CoA from the MCAD-$FADH_2$−octenoyl-CoA charge-transfer complex, CT_2 (via the facile pathway), by acetoacetyl-CoA (Panel A), IACoA (Panel B), and octenoyl-CoA (panel C). Panel A: The after-mixing concentrations of CT_2 and acetoacetyl-CoA were 5 and 500 μM, respectively. The solid smooth line is the best fit of the experimental data for a single-exponential rate law, with a rate constant of 7.1 s^{-1}. Panel B: The after-mixing concentrations of CT_2 and IACoA were 5 and 250 μM, respectively. The solid smooth line is the best fit of the experimental data for a single-exponential rate law, with a rate constant of 5.4 s^{-1}. Panel C: The after-mixing concentrations of CT_2 and octenoyl-CoA were 5 and 50 μM, respectively. The solid smooth line is the best fit of the experimental data for a single-exponential rate law, with a rate constant of 3.8 s^{-1}.

variations in the observed rate constants when different CoA ligands (viz., acetoacetyl-CoA, IACoA, and octenoyl-CoA) are employed as competing ligands during these experiments (see below). We also examined the kinetic profile for the reaction of CT_2 with octenoyl-CoA via transient kinetic methods. This profile was important in assessing the feasibility of alternative pathways for the entrance of octenoyl-CoA into the reaction scheme (see Discussion). Figure 3C shows the time-dependent increase in absorption at 450 nm upon mixing 10 μM CT_2 (generated upon mixing 10 μM MCAD-FAD and 12 μM octanoyl-CoA) with 100 μM octenoyl-CoA via the stopped-flow syringes (the after-mixing concentrations of CT_2 and octenoyl-CoA are 5 and 50 μM, respectively). The reaction trace was best fitted by a single-exponential rate equation, with a rate constant of 3.8 ± 0.02 s^{-1}. It should be pointed out that this observed rate constant is 2-fold lower than those obtained from the data of Figure 3A,B. However, considering the added complexity of the reaction pathways of MCAD-FAD + octenoyl-CoA interaction (vis-à-vis MCAD-FAD + acetoacetyl-CoA/IACoA interactions), this difference is not significant (see above). Like those of other CoA ligands, the observed relaxation rate constant remained unchanged

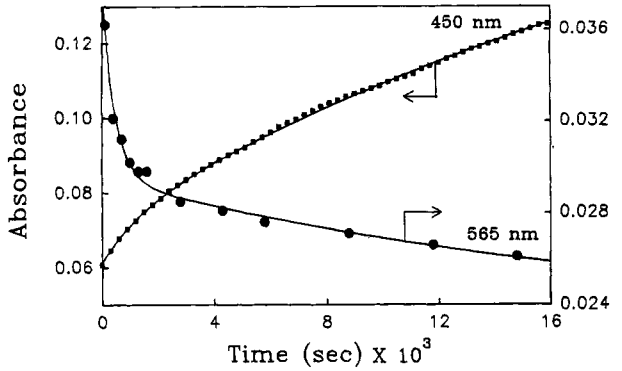

FIGURE 4: Comparative kinetic profiles for the dissociation of octenoyl-CoA from CT_2 (via the restricted pathway; 565-nm trace) and the oxidase reaction of the enzyme (450-nm trace). Solid circles represent absorptions at 565 nm (taken from the time-dependent spectral changes) upon incubation of 10 μM MCAD-FAD with 100 μM octanoyl-CoA under anaerobic conditions. Solid squares represent the time-dependent absorption changes at 450 nm upon incubation of 10 μM MCAD-FAD with 8 μM octanoyl-CoA under aerobic conditions (i.e., in the presence of 240 μM buffer-dissolved oxygen). To show the fitted curve (solid smooth line), only selected absorption points (solid squares) are shown at 450 nm. The solid smooth lines are the best fits of the experimental data according to the biphasic rate equations for the fast and slow rate constants of 2.18×10^{-3} and 5.2×10^{-5} s^{-1}, respectively, for the data at 565 nm, and 7.1×10^{-4} and 3.54×10^{-5} s^{-1} for the data at 450 nm.

upon increasing the concentration of octenoyl-CoA at least by 3-fold (eq 13).

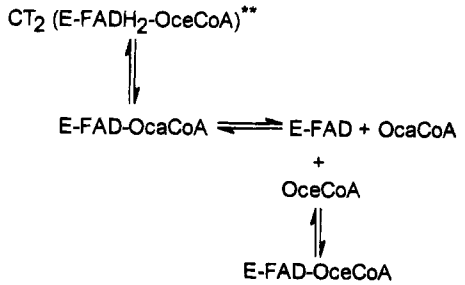

(13)

In summary, all three CoA ligands (viz., acetoacetyl-CoA, IACoA, and octenoyl-CoA) cause the reversal of the octanoyl-CoA-dependent reductive half-reaction of the enzyme (eqs 11−13), and the overall rate constant for this reaction varies between 3.8 and 7.1 s^{-1}.

Effect of High Concentrations of Octanoyl-CoA on the Stability of the MCAD-FADH$_2$−Octenoyl-CoA Charge-Transfer Complex (CT_2). We examined the effect of high concentrations of octanoyl-CoA on the spectral properties of CT_2. As expected, octanoyl-CoA, being a substrate of the enzyme, did not cause the return of the oxidized-flavin spectrum (i.e., via reversal of the reductive half-reaction of the enzyme) as observed with other CoA ligands (see Figures 1−3 and eqs 11−13). Instead, the charge-transfer band of CT_2 slowly disappeared in the presence of a high concentration of octanoyl-CoA. Figure 4 (565 nm trace) shows the time-dependent decrease in absorbance at 565 nm when 10 μM MCAD-FAD is incubated with 100 μM octanoyl-CoA under strictly anaerobic conditions. The time-dependent reaction profile is best fitted by a biphasic rate equation, with observed fast and slow rate constants of 2.18×10^{-3} and 5.2×10^{-5} s^{-1}, respectively. The amplitudes of the fast and slow phases are 21 and 16% of the total amplitude for a complete decay of the charge-transfer band. We observed that when the octanoyl-CoA concentration is increased from 100 to 500 μM, the observed rate constant for the fast phase decreased by a factor of 3 (due to the decreased contributions of the reverse rate constants; Bernasconi, 1976). Under similar conditions, the amplitude of the fast phase increased to 35%. A qualitatively similar result was found for the decay of the charge-transfer complex band (formed upon incubation of MCAD-FAD with IPCoA) in the presence of an excessive concentration of IPCoA (Johnson & Srivastava, 1993). These observations led us to propose that, in the presence of octanoyl-CoA, CT_2 is converted into MCAD-FADH$_2$ + octenoyl-CoA via formation of the MCAD-FADH$_2$−octenoyl-CoA Michaelis complex. (As will be elaborated in a subsequent communication, the latter complex is kinetically as well as electronically different from the contemporary charge-transfer complexes.) This reaction is driven by complexation of MCAD-FADH$_2$ with octanoyl-CoA (present in an excessive concentration; eq 14).

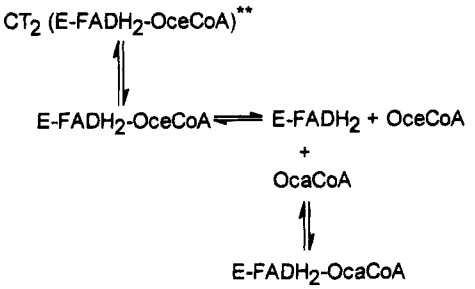

(14)

Since the slow phase of the octanoyl-CoA-dependent reaction (Figure 4) has a half-life of about 3.7 h, it takes about 11 h to complete 88% of the (slow-phase associated) reaction. At the end of this time period, about 20% of the enzyme is found to be inactive (data not shown). A similar loss of the enzyme activity is noted during the course of the oxidase reaction (see below). These added with the fact that neither the rate constant nor the amplitude of the slow phase shows any predictable dependence on octanoyl-CoA (data not shown) led us to suspect that the origin of the slow phase lies in the thermal instability of the enzyme. Consequently, the slow phase is not taken into consideration toward further mechanistic deductions.

Oxidation of MCAD-FADH$_2$−Octenoyl-CoA Charge-Transfer Complex (CT_2). With the precedent of our earlier observation that the decay of the charge-transfer complex (formed with IPCoA; Johnson & Srivastava, 1993) limits the overall rate of the oxidase reaction (Johnson & Srivastava, 1993), we proceeded to inquire whether the oxidase reaction of the enzyme (involving octanoyl-CoA as substrate) adheres to the same mechanistic principle(s) or not. Since the oxidase reaction of the enzyme is considerably slower with octanoyl-CoA as substrate, this reaction was examined under the condition [MCAD-FAD] > [octanoyl-CoA]. Under this condition, the repetitive turnover of the enzyme would be avoided. Like others, we also noted that the charge-transfer band formed upon incubation of MCAD-FAD and octanoyl-CoA slowly disappeared with a concomitant appearance of the oxidized flavin band under aerobic conditions. In Figure 4, the 450-nm trace shows the time-dependent reaction profile for the increase in absorption at 450 nm when a mixture of 10 μM MCAD-FAD and 8 μM octanoyl-CoA reacts with 240 μM buffer-dissolved O_2 as the electron acceptor. This reaction trace is best fitted by a double-exponential rate equation, with fast and slow rate constants of 7.1×10^{-4} and 3.54×10^{-5} s^{-1}, respectively. Note that these rate

Scheme 1

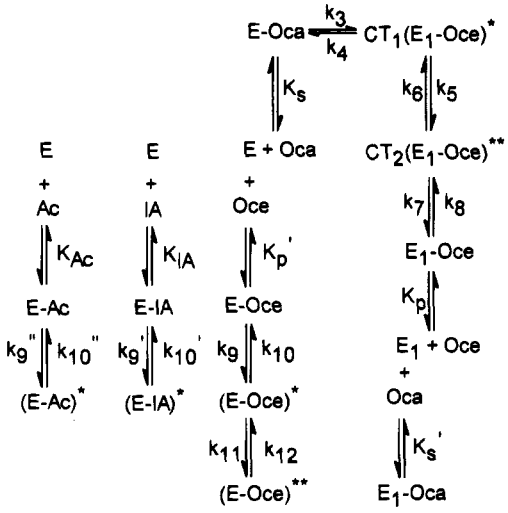

E = MCAD-FAD; E_1 = MCAD-$FADH_2$

Oca = Octanoyl-CoA; Oce = Octenoyl-CoA

Ac = Acetoacetyl-CoA; IA = IACoA

constants are similar to those obtained for the displacement of octenoyl-CoA from CT_2 in the presence of an excessive concentration of octanoyl-CoA (Figure 4, 565-nm trace). These observations are consistent with the fact that the oxidase activity originates concomitantly with the decay of the MCAD-$FADH_2$–octenoyl-CoA charge-transfer complex CT_2. However, unlike the octanoyl-CoA-dependent decay of CT_2, the oxidase reaction is expected to yield a biphasic kinetic profile. This is because the second rate constant for the oxidation of MCAD-$FADH_2$ by O_2 (2.65×10^3 M^{-1} s^{-1}; Johnson et al., 1994) is at least 5 orders of magnitude lower than the diffusion-limited rate constants for the association of CoA ligands with the enzyme. Thus, the kinetic drive in the presence of 240 μM buffer-dissolved oxygen would be significantly weaker than that obtained for the (diffusion limited) association of enzyme with CoA ligands. Therefore, the two slower steps (viz., $CT_2 \rightleftharpoons$ MCAD-$FADH_2$–octenoyl-CoA and the oxidation of MCAD-$FADH_2$ by O_2) are expected to yield a biphasic relaxation profile, as observed during the course of the oxidase reaction. However, we must admit that we do not understand, at this time, the molecular basis for the origin of the slow phase during the octanoyl-CoA-dependent disappearance of the charge-transfer complex band.

DISCUSSION

A cumulative account of all the experimental results presented in the earlier section, as well as those published previously (Johnson et al., 1992; Johnson & Srivastava, 1993; Kumar & Srivastava, 1994), leads us to formulate a comprehensive model for the octanoyl/octenoyl-CoA-dependent MCAD-catalyzed reaction and the interaction of other CoA-ligands with MCAD (Scheme 1). As per this scheme, whereas the octanoyl/octenoyl-CoA-dependent processes (chemical as well as physical interactions) involve three steps (i.e., binding followed by two isomerizations; Kumar & Srivastava, 1994), IACoA and acetoacetyl-CoA-dependent interactions involve only two steps (Johnson et al., 1992). In Scheme 1, we differentiate between the MCAD-$FADH_2$–octenoyl-CoA charge-transfer complexes (e.g., CT_1 and CT_2) from the MCAD-$FADH_2$–octenoyl-CoA collision/Michaelis complex. As will be published subsequently, the MCAD-$FADH_2$–octenoyl-CoA collision/Michaelis complex does not exhibit the property of the charge transfer complex band.

Due to an apparent zero-order concentration dependencies of the relaxation rate constants on the ligand concentrations (under pseudo-first-order conditions), we were not able to determine the microscopic rate and equilibrium constants for the individual steps of Scheme 1 by analytical methods (Bernasconi, 1976). Recourse was made to determine the above parameters by numerical methods (Betts & Srivastava, 1991). Assuming that the enzyme–ligand binding steps are the diffusion-limited processes, with an association rate constant of 1×10^9 M^{-1} s^{-1} (Hammes, 1982), we simulated the model of Scheme 1 under our experimental conditions (see Table 1). During this simulation, we utilized dissociation constants for the MCAD-FAD–octanoyl-CoA complex of 1.53 μM (based on the reverse titration results of Figure 1) and for the MCAD-FAD–octenoyl-CoA collision/Michaelis complex of 3.28 μM. The latter estimate is based on our recent determination of the dissociation constant of the stable form of the (MCAD-FAD–octenoyl-CoA)** complex as 0.41 μM (our unpublished results). This dissociation constant is composed of a binding steps (K_d = 3.28 μM) and two isomerization steps ($K_{isomerization}$ = 1/8) (Kumar & Srivastava, 1994). While simulating the pathway for the decay of CT_2 in the presence of an excessive concentration of octanoyl-CoA (eq 14), we realized that both rates and equilibrium parameters would be predicted best if the dissociation constant of the MCAD-$FADH_2$–octenoyl-CoA Michaelis-complex and the overall dissociation constant of the MCAD-$FADH_2$–octanoyl-CoA complex (which may include binding followed by subsequent isomerization) are taken as 10 μM and 2 nM, respectively. The relative magnitudes of these parameters are comparable to those determined for enzyme–IPCoA/IACoA interactions (Johnson et al., 1992; Johnson & Srivastava, 1993; Johnson et al., 1994).

Table 1 summarizes the experimentally observed relaxation rate constants vis-a-vis those obtained from the numerical simulations of the corresponding reactions under identical experimental conditions. The rate and equilibrium constants utilized during these simulations are presented at the bottom of Table 1. Note a remarkable correspondence between the relaxation rate constants observed experimentally and those determined from the simulated traces (see Materials and Methods).

Energetics of the Octanoyl-CoA-Dependent Reductive Half-Reaction of the Enzyme. The rate and equilibrium constants derived from the numerical simulation results of Table 1 allowed us to construct the Gibbs' free energy profile for the octanoyl-CoA-dependent reductive half-reaction of the enzyme (Figure 5). This profile is based on the standard states of octanoyl-CoA and octenoyl-CoA as being 1 M. The Gibbs' free energy for the MCAD-FAD (reference state) is taken as being zero. As per the free energy profile of Figure 5, the second charge-transfer complex (CT_2) is the most stable enzyme species. Given that the difference in Gibbs' free energy between CT_2 and MCAD-FAD + octanoyl-CoA is 9.9 kcal/mol and that between CT_2 and MCAD-$FADH_2$ + octenoyl-CoA is 15.6 kcal/mol, the conversion of CT_2 to MCAD-FAD + octanoyl-CoA is about 5.7 kcal/mol more favorable thermodynamically than the conversion of CT_2 to

Table 1: Comparison between Experimentally Determined and Simulated Relaxation Rate Constants[a]

reaction[b]	kinetic profile[c]	relaxation rate constants (s^{-1}) observed	simulated
^{1}E-FAD + OcaCoA ⇌ CT_2	biphasic	$1/\tau_1 = 649$	$1/\tau_1 = 690$
		$1/\tau_2 = 66.5$	$1/\tau_2 = 78.4$
^{2}E-FAD + OceCoA ⇌ (E-FAD-OceCoA)**	biphasic	$1/\tau_1 = 661$	$1/\tau_1 = 705$
		$1/\tau_2 = 26.2$	$1/\tau_2 = 41.1$
^{3}E-$FADH_2$ + OceCoA ⇌ (E-FAD-OceCoA)**	biphasic	$1/\tau_1 = 757$	$1/\tau_1 = 752$
		$1/\tau_2 = 3.5$	$1/\tau_2 = 4.8$
$^4CT_2$ + OcaCoA ⇌ E-$FADH_2$-OcaCoA	monophasic[d]	$1/\tau = 2.18 \times 10^{-3}$	$1/\tau = 2.7 \times 10^{-3}$
$^5CT_2$ + OceCoA ⇌ (E-FAD-OceCoA)**	monophasic	$1/\tau = 3.8$	$1/\tau = 6.6$
$^6CT_2$ + IACoA ⇌ (E-FAD-IACoA)*	monophasic	$1/\tau = 5.4$	$1/\tau = 8.5$

[a] For different segments of reaction Scheme 1. The rate and equilibrium constants used during simulations are as follows: $K_s = 1.53$ μM; $k_3 = 400$ s^{-1}; $k_4 = 300$ s^{-1}; $k_5 = 150$ s^{-1}; $k_6 = 7$ s^{-1}; $k_7 = 3 \times 10^{-4}$ s^{-1}; $k_8 = 800$ s^{-1}; $K_p = 10$ μM; $K_s' = 2$ nM; $K_p' = 3.28$ μM; $k_9 = 400$ s^{-1}; $k_{10} = 300$ s^{-1}; $k_{11} = 60$ s^{-1}; $k_{12} = 10$ s^{-1}. [b] Reaction conditions for the observed and simulated traces (1−6) are as follows: (1) MCAD-FAD = 0.75 μM, OcaCoA = 40 μM; (2) MCAD-FAD = 5 μM, OceCoA = 150 μM; (3) MCAD-$FADH_2$ = 5 μM, OceCoA = 250 μM; (4) MCAD-FAD = 10 μM, OcaCoA = 100 μM; (5) MCAD-$FADH_2$−OceCoA = (5 μM MCAD-FAD + 6 μM OcaCoA), OceCoA = 50 μM, (6) MCAD-$FADH_2$−OceCoA = (5 μM MCAD-FAD + 5.5 μM OcaCoA), IACoA = 250 μM. [c] The experimental or simulated results were analyzed according to single-exponential (monophasic) or double-exponential (biphasic) rate laws. [d] The second slow phase ($t_{1/2}$ = 3.7 h) is not considered.

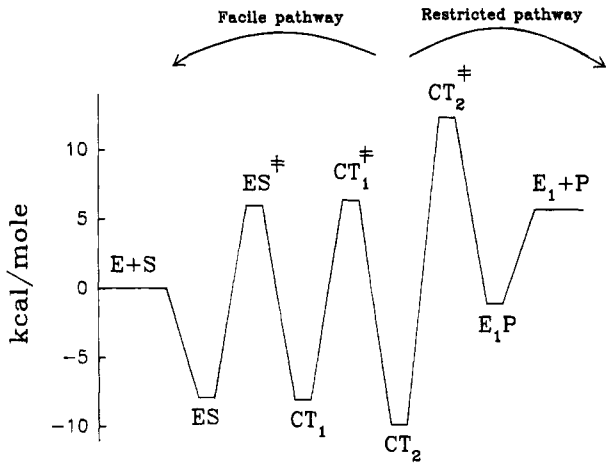

FIGURE 5: The Gibbs' free energy profile for the octanoyl-CoA-dependent reductive half-reaction of the enzyme. E, S, E_1, and P represent MCAD-FAD, octanoyl-CoA, MCAD-$FADH_2$, and octenoyl-CoA, respectively. The overall profile is constructed for the rates and dissociation constants given at the bottom of Table 1, according to the thermodynamic relationships given in Materials and Methods. Note the energetic basis for the assignment of the facile and restricted pathways for the dissociation of octenoyl-CoA.

MCAD-$FADH_2$ + octenoyl-CoA. Furthermore, the highest energy barrier for the conversion of CT_2 to MCAD-FAD + octanoyl-CoA is 16.3 kcal/mol, whereas that for the conversion of CT_2 to MCAD-$FADH_2$ + octenoyl-CoA is 22.2 kcal/mol. Clearly, the reversal of the reductive half-reaction of the enzyme (i.e., CT_2 → MCAD-FAD + octanoyl-CoA) is preferred over the conversion of CT_2 to MCAD-$FADH_2$ + octenoyl-CoA, both kinetically as well as thermodynamically. On the basis of these energetic consequences, these pathways are formally assigned as being the facile and restricted pathways, respectively.

Is the Gibbs' free energy profile of Figure 5 consistent with the difference in free energies of the selected enzyme species, predictable on the basis of the redox potential measurements? Toward this end, we note that the redox potential of the octenoyl-CoA/octanoyl-CoA pair (−41 mV), as well as that of MCAD-FAD in the absence (−145 mV) and presence (−26 mV) of bound octanoyl/octenoyl-CoA, have been determined (Lenn et al., 1990; Johnson & Stankovich, 1993). On the basis of these estimates, the free energy changes for MCAD-FAD + octanoyl-CoA ⇌ MCAD-$FADH_2$ + octenoyl-CoA and MCAD-FAD−octanoyl-CoA ⇌ MCAD-$FADH_2$−octenoyl-CoA would be calculated to be 4.8 kcal/mol and 1.2 kcal/mol, respectively. These values are 0.86 and 0.78 kcal/mol lower than those obtained from the free energy profile of Figure 5. At this point, we are uncertain whether the above discrepancy lies in small errors introduced during measurements of redox potentials of one or the other species or during our own estimates of the rate and equilibrium constants, or both. For example, a recent refinement of the redox potential of the enzyme from −136 mV (Lenn et al., 1990) to −145 mV (Johnson & Stankovich, 1993) accounts for a difference in free energy of 0.42 kcal/mol. A similar magnitude of difference in free energy can be expected if one of our rate or dissociation constant measurements is off by 2-fold. Hence, considering such potential errors, it is evident that the energetic predictions made on the basis of our kinetic measurements are not too different from those made on the basis of redox potential measurements.

Origin of the Oxidase Activity of the Enzyme. Unlike the CoA ligands, viz., acetoacetyl-CoA, IACoA, and so on, an excessive concentration of octanoyl-CoA promotes the "direct" dissociation of octenoyl-CoA from the reduced enzyme site (i.e., via the restricted pathway). This is accomplished by formation of the MCAD-$FADH_2$−octanoyl-CoA complex and is evident by a slow disappearance of the reduced enzyme−octenoyl-CoA charge transfer complex band (Figure 4, 565-nm trace). As compared to the facile pathway, this pathway is relatively less favorable both thermodynamically and kinetically, and thus it is referred to as the restricted pathway.

The fact that the kinetic profile for the disappearance of the charge transfer complex band via the restricted pathway (Figure 4, 565-nm trace) is similar to that obtained for the oxidation of the reduced enzyme (Figure 4, 450-nm trace) implies that the oxidase reaction of the enzyme remains suppressed as long as the enzyme exists in the charge-transfer complex, CT_2. Alternatively, the oxidase reaction of the enzyme originates concomitantly with the rate of decay of the charge-transfer complex. This suggests that the enzyme species which is directly oxidized by O_2 is either the MCAD-$FADH_2$−octenoyl-CoA Michaelis complex or MCAD-$FADH_2$, or both. Of these, it is well known that MCAD-$FADH_2$ is directly oxidized by O_2 (Johnson et al., 1994). The question arises whether or not the MCAD-$FADH_2$−

octenoyl-CoA Michaelis complex is also oxidized by O_2. Unfortunately, our present kinetic data (involving octanoyl-CoA/octenoyl-CoA as substrate/product pair of the enzyme) cannot resolve this issue. However, while investigating the IPCoA-dependent reactions, we realized that the steady-state kinetic parameters of the oxidase reaction could be rationalized best if MCAD-$FADH_2$ was taken to be the only oxidizable enzyme species. Such steady-state kinetic experiments could not be performed with octanoyl-CoA as enzyme substrate, due to the instability of reagents (on a longer time scale) employed for measuring the oxidase reaction of the enzyme involving nonchromogenic acyl-CoA substrates (Johnson et al., 1992). Hence, unlike our demonstration with the IPCoA/IACoA pair (Johnson et al., 1994), we cannot emphasize that the MCAD-$FADH_2$−octenoyl-CoA Michaelis complex is not a substrate for the enzyme-catalyzed oxidase reaction. Nevertheless, in the case of both these substrates (viz., IPCoA and octanoyl-CoA), it is absolutely clear that the reduced flavins of the corresponding MCAD-$FADH_2$−enoyl-CoA charge-transfer complexes are not oxidized by O_2 and that the oxidase reaction of the enzyme (involving IPCoA and octanoyl-CoA as substrates) occurs following the decay of the corresponding charge-transfer complexes. Hence, the mechanistic principle for the origin of the oxidase activity remains unchanged irrespective of whether the substrate is "good" (e.g., octanoyl-CoA) or "poor" (e.g., IPCoA).

In this regard, we note that Choong and Massey (1980) demonstrated that the rate of oxidation of flavin semiquinone (bound to lactate oxidase) is suppressed in the presence of pyruvate (the reaction product of the enzyme). To probe whether this suppression is due to the slow oxidation of the enzyme−semiquinone−pyruvate complex itself or not, these authors compared the dissociation "off rate" of pyruvate from the above complex with the rate constant for the oxidase reaction. Given that the off rate constant for pyruvate (from the enzyme−semiquinone−pyruvate complex; 3.85×10^{-4} s^{-1}) precisely matched the specific rate constant for the oxidase reaction (3.2×10^{-4} s^{-1}), Choong and Massey concluded that the enzyme−semiquinone is the only enzyme species which is oxidized by O_2. Hence, the oxidation of the lactate oxidase−semiquinone−pyruvate complex must proceed via dissociation of pyruvate from the enzyme site. It should be pointed out that, in contrast to our view (see above) as well as the experimental results of Choong and Massey (1980), Wang and Thorpe (1991) maintain that the suppression of the oxidase reaction of MCAD-$FADH_2$ by CoA ligands is due to the slow oxidations of the corresponding MCAD-$FADH_2$−ligand complexes.

In summary, it appears evident that one of the most important aspects of MCAD catalysis is the stabilization of the reduced enzyme−enoyl-CoA charge-transfer complex. The latter complex promotes the dehydrogenase reaction by transferring the electrons (from the reduced flavin) directly to the "organic" electron acceptors (e.g., ETF) (Johnson et al., 1993, and our unpublished results) as well as suppresses the oxidase reaction of the enzyme by precluding the reduction of oxygen. Given that both octanoyl-CoA and octenoyl-CoA (or other CoA ligands) destabilize the charge-transfer complex (via facile and restricted pathways), it is imperative that this enzyme must function (in the physiological milieu) under limited concentrations of the free substrates and products, as well as other CoA ligands.

REFERENCES

Beinert, H. (1963a) *Enzymes (2nd Ed.) 7*, 447−466.
Beinert, H. (1963b) *Enzymes (2nd Ed.) 7*, 467−476.
Beinert, H., & Page, E. (1957) *J. Biol. Chem. 225*, 479−497.
Bernasconi, C. F. (1976) *Relaxation Kinetics*, Academic Press, New York.
Bernert, J. T., & Sprecher, H. (1977) *J. Biol. Chem. 252*, 6737−6744.
Betts, G. F., & Srivastava, D. K. (1991) *J. Theor. Biol. 151*, 155−167.
Choong, Y. S., & Massey, V. (1980) *J. Biol. Chem. 255*, 8672−8677.
Engel, P. C. (1990) *Chemistry and Biochemistry of Flavoenzymes* (Muller, F., Ed.) Vol. III, pp 597−655, CRC Press, Inc., London.
Fersht, A. R. (1985) *Enzymes Structure and Mechanism*, 2nd ed., W. H. Freeman, Co., San Francisco and Oxford.
Frerman, F. E., Miziorko, H. M., & Beckmann, J. D. (1980) *J. Biol. Chem. 255*, 11192−11198.
Ghisla, G., Thorpe, C., & Massey, V. (1984) *Biochemistry 23*, 3154−3161.
Hall, C. L., Lambeth, J. D., & Kamin, H. (1979) *J. Biol. Chem. 254*, 2023−2031.
Hammes, G. G. (1982) *Enzyme Catalysis and Regulation*, Academic Press, New York.
Johnson, B. D., & Stankovich, M. T. (1993) *Biochemistry 32*, 10779−10785.
Johnson, J. K., & Srivastava, D. K. (1993) *Biochemistry 32*, 8004−8013.
Johnson, J. K., Wang, Z. X., & Srivastava, D. K. (1992) *Biochemistry 31*, 10564−10575.
Johnson, J. K., Kumar, N. R., & Srivastava, D. K. (1993) *Biochemistry 32*, 11575−11585.
Johnson, J. K., Kumar, N. R., & Srivastava, D. K. (1994) *Biochemistry 33*, 4738−4744.
Kumar, N. R., & Srivastava, D. K. (1994) *Biochemistry 33*, 8833−8841.
Lau, S.-M., Brantley, R. K., & Thorpe, C. (1989) *Biochemistry 28*, 8255−8262.
Lehman, T. C., & Thorpe, C. (1990) *Biochemistry 29*, 10954−10601.
Lenn, N. D., Stankovich, M. T., & Liu, H. (1990) *Biochemistry 29*, 3709−3715.
Schopfer, L. M., Massey, V., Ghisla, S., & Thorpe, C. (1988) *Biochemistry 27*, 6599−6611.
Srivastava, D. K., Kumar, N. R., & Peterson, K. L. (1995) *Biochemistry 34*, 4625−4632.
Thorpe, C., Matthews, R. G., & Williams, C. H., Jr. (1979) *Biochemistry 18*, 331−337.
Wang, R., & Thorpe, C. (1991) *Biochemistry 30*, 7895−7901.
Wang, Z. X., Kumar, N. R., & Srivastava, D. K. (1992) *Anal. Biochem. 206*, 376−381.

BI950417V